

Supplementary Information

Lanthanum Modified Biochar Particles Derived from Municipal Sludge: Preparation and mechanisms for phosphate recovery

Jingshi Pan^{a,b,c}, Haiyan Yang^{a,b*}, Lei Liu^d, Biqing Li^c, Xia Tang^c, Xuewei Wu^c, Liguozhang^{a,b*}, Guang-Guo Ying^{a,b}

^a Guangdong Provincial Key Laboratory of Chemical Pollution and Environmental Safety & MOE Key Laboratory of Theoretical Chemistry of Environment, South China Normal University, Guangzhou 510006, China

^b School of Environment, South China Normal University, Guangdong Provincial Engineering Technology Research Center for Wastewater Management and Treatment, University Town, Guangzhou 510006, China

^c Guangzhou Sewage Purification Co. Ltd., Guangzhou 510655, China

^d School of Environment and Civil Engineering, Dongguan University of Technology, Dongguan 523808, China

*Corresponding author.

E-mail address: haiyan.yang@m.scnu.edu.cn; zhanglg@scnu.edu.cn;

Contents

Section S1 Characterization of SBP and SBP-La

Section S2 Preparation of anaerobic digestion liquid

Section S3 Batch adsorption experiments procedures and modelling

Table S1 Classification of ecological risk level based on Ei and RI^1

Table S2 Water quality of municipal wastewater and anaerobic digestion liquid of sludge

Table S3 Major elements of SBP and SBP-La measured by SEM-EDS

Table S4 Physical properties of SBP and SBP-La

Table S5 Leachable heavy metals from SBP and SBP-La in batch experiments ($\mu\text{g/L}$)

Table S6 Kinetic curve fitting parameters for phosphate adsorption on SBP and SBP-La

Table S7 Isotherm curve fitting parameters for phosphate adsorption on SBP and SBP-La

Table S8 Thermodynamic curve fitting parameters for phosphate adsorption on SBP and SBP-La

Fig. S1 Fractions of phosphate species at different pH.²

Fig. S2 XPS full spectrum of SBP (a) and SBP-La (b) before and after phosphate adsorption.

Text S1

Characterization of SBP and SBP-La

The physicochemical properties of SBP and SBP-La were analyzed before and after phosphate adsorption. BET surface area was detected by a Micromeritics ASAP 2046 surface area analyzer (Micromeritics Co., U.S.). The gas adsorption isotherm (N_2 , 77.30 K) was used. Scanning electron microscope (SEM) (ZEISS Ultra 55, German) with Energy Dispersive Spectroscopy (EDS) line scanning was applied to determine biochar surface morphology and element compounds. The powder X-ray diffraction (XRD) (Ultima IV, Japan) was used to identify the material crystalline phases. Fourier transform infrared spectrometer (SepctrumTwo, Germany) was employed to identify surface functional groups of materials with a wave number range of 400-4000 cm^{-1} . Zeta potentials at a series of pH values were measured to determine the zero charge point (pH_{PZC}) of biochar sample (Zetasizer Nano ZS90, Malvern Instruments, United Kingdom). The coordination environment of La was investigated by an X-ray photoelectron spectrometer (ThermoFisher 3600, U.K.) with CuKa irradiation (40 kV, 30 mA).

Text S2

Preparation of anaerobic digestion liquid

After collecting from anaerobic tank from a WWTP in Guangzhou, the sludge was settled down overnight and anaerobically digested in a shaking incubator (180 rpm) at 37 °C for 15 days. The liquid phase (supernatant) was collected from the fermented sludge solution by centrifugation (6000 rpm) for 20 min.

Text S3

Batch adsorption experiments procedures and modelling

Batch experiments were conducted by adding 20.0 mg of SBP or SBP-La into 25.0 mL of

phosphate (50.0 mg P/L) solution (pH 5.0) in 50 mL centrifuge tubes, The effects of material dosage and solution pH on phosphate adsorption were tested by varying the biochar dosages from 0.4 g/L to 6.0 g/L and varying pH from 3 to 11 (adjusting by 0.1 mol/L NaOH and 0.1 mol/L HCl), respectively. Meanwhile, a set of experiments were carried out to study the influence of coexisting anions (50.0 and 100.0 mg/L), including nitrate (NO_3^-), chloride (Cl^-), sulfate (SO_4^{2-}), and bicarbonate (HCO_3^-), on phosphate adsorption by biochar. Additionally, adsorption kinetics were investigated by collecting samples in suspensions at different predetermined time intervals (1-24 h). Phosphate adsorption isotherms were studied by changing initial phosphate concentrations (5–250 mg/L), in which samples were collected after reaching equilibrium (24 h). Phosphate adsorption was also conducted at 25, 35 and 45 °C (298.15, 308.15 and 318.15 K) to investigate adsorption thermodynamics.

Kinetics, isotherm, and thermodynamic models For adsorption kinetics, pseudo first-order model, pseudo second-order model and intra-particle diffusion model were commonly used to describe kinetics process. The pseudo first-order model and pseudo second-order model equations are given as:³

$$\lg(q_e - q_t) = \lg q_e - k_1 t \quad (\text{S1})$$

$$\frac{t}{q_t} = \frac{1}{k_2 q_e^2} + \frac{t}{q_e} \quad (\text{S2})$$

where q_t (mg/g) is the phosphate adsorption capacity at time t . k_1 (h) and k_2 ($\text{g} \cdot \text{mg}^{-1} \cdot \text{h}^{-1}$) are the rate constants of pseudo first-order and pseudo second-order adsorption, respectively.

The equation (S3) is the intra-particle diffusion equation:

$$q_t = k_s t^{1/2} + C \quad (\text{S3})$$

where k_s ($\text{mg} \cdot \text{g}^{-1} \cdot \text{h}^{1/2}$) and C are the adsorption rate constant and intercept of the model, respectively.

Additionally, the kinetics data were also fitted to Weber-Morris model to study the possible effect of intra-particle diffusion on anion adsorption process. Weber-Morris model (linear form) is given in Equation (S4):⁴

$$q_t = k_1 t^{\frac{1}{2}} + C \quad (S4)$$

Where q_t was capacity of adsorbed contaminant at time t (h), k_i and C were the intra-diffusion rate constant ($\text{mg} \cdot \text{g}^{-1} \cdot \text{h}^{-0.5}$) and the intercept of the boundary layer thickness, respectively.

Meanwhile, Langmuir and Freundlich patterns are used to describe phosphate adsorption isotherms. The equations are expressed as equation (S5) and (S6), respectively.^{5,6}

$$\frac{C_e}{q_e} = \frac{1}{Q_0 K_L} + \frac{C_e}{Q_0} \quad (S5)$$

$$\lg q_e = \lg K_F + \frac{\lg C_e}{n} \quad (S6)$$

where Q_0 (mg/g) is the maximum phosphate adsorption capacity estimated by Langmuir model, in which K_L (mg/L) represents Langmuir equilibrium constant relating to the adsorption energy. In equation (S6), K_F ($(\text{mg/g})(\text{mg/L})^{1/n}$) represents the adsorption affinity, and n is the indicator for adsorbent surface heterogeneity.

For thermodynamic study, Gibbs Free Energy was applied to determine the properties of adsorption process, in which the equations are given as:

$$\Delta G_0 = -RT \ln K \quad (S7)$$

$$\ln K = \frac{\Delta S_0}{R} - \frac{\Delta H_0}{RT} \quad (S8)$$

Where ΔG_0 (KJ/mol) represents the change of Gibbs free energy. R (8.314 J/(mol·K)) and K (Q_e / C_e) are the thermodynamic constants at absolute temperature T (K). The ΔS_0 (J/(mol·K)) and ΔH_0 (KJ/mol) are reaction entropy and enthalpy, respectively.

Table S1Classification of ecological risk level based on E_i and RI ¹

| E_i | RI | Risk level |
|-----------|------------|-------------------|
| ≤ 40 | ≤ 150 | low risk |
| 41-80 | 151-300 | moderate risk |
| 81-160 | 301-600 | considerable risk |
| 161-320 | 601-1200 | high risk |
| > 320 | > 1200 | very high risk |

Table S2

Water quality of municipal wastewater and anaerobic digestion liquid of sludge

| Parameters of water quality (unit) | Municipal wastewater | anaerobic digestion liquid of sludge |
|---------------------------------------|----------------------|---|
| pH (/) | 6.56 | 7.02 |
| ORP (mV) | -35.0 | -239 |
| SCOD (mg/L) | 34.4 | 274 |
| PO_4^{3-} (mg/L) | 4.97 | 55.1 |
| NH_4^+ (mg/L) | 8.61 | 274 |
| SO_4^{2-} (mg/L) | 26.3 | 7.75 |
| Cl^- (mg/L) | 30.7 | 12.5 |
| NO_3^- (mg/L) | 5.74 | 1.19 |
| HCO_3^- (mg/L) | 224 | 1205 |

Table S3

Major elements of SBP and SBP-La measured by SEM-EDS

| Element | Contents/% | |
|---------|----------------|--------|
| | SBP | SBP-La |
| C | 32.74 | 36.28 |
| O | 44.22 | 30.74 |
| Si | 8.42 | 4.65 |
| Ca | 4.56 | 0.80 |
| Al | 2.60 | 1.64 |
| Fe | 1.51 | 0.84 |
| S | 1.31 | 0.37 |
| Mg | 0.61 | 0.38 |
| P | 1.17 | -- |
| La | - ^a | 13.52 |

^a Not detected**Table S4**

Physical properties of SBP and SBP-La

| sample | Surface area (m ² /g) | Pore | Average pore size (nm) |
|-----------------------|---------------------------------------|-------------------------------|-----------------------------|
| | | volume (cm ³ /g) | |
| SBP | 19.2 | 0.0462 | 9.64 |
| SBP-P ^a | 23.2 | 0.0540 | 9.37 |
| SBP-La | 6.49 | 0.0141 | 8.67 |
| SBP-La-P ^a | 39.9 | 0.0617 | 6.19 |

^a SBP or SBP-La samples after phosphate adsorption.

Table S5Leachable heavy metals from SBP and SBP-La in batch experiments ($\mu\text{g/L}$)

| | pH | As | Cd | Cu | Ni | Pb | Zn |
|------|--------|-------|-------|-------|-------|-------|-------|
| 3.0 | SBP | 72.71 | 15.08 | 18.89 | 11.87 | 19.15 | 51.79 |
| | SBP-La | 79.59 | 15.08 | 18.89 | 11.86 | 19.13 | 51.83 |
| 5.0 | SBP | 72.69 | 15.08 | 18.89 | 11.87 | 19.15 | 51.83 |
| | SBP-La | 76.99 | 15.08 | 18.89 | 11.86 | 19.14 | 51.83 |
| 7.0 | SBP | 72.69 | 15.08 | 18.89 | 11.87 | 19.16 | 51.79 |
| | SBP-La | 76.53 | 15.08 | 18.89 | 11.86 | 19.17 | 51.83 |
| 9.0 | SBP | 72.69 | 15.08 | 18.89 | 11.87 | 19.15 | 51.82 |
| | SBP-La | 76.46 | 15.08 | 18.89 | 11.86 | 19.14 | 51.83 |
| 11.0 | SBP | 72.69 | 15.08 | 18.89 | 11.87 | 19.15 | 51.80 |
| | SBP-La | 76.90 | 15.08 | 18.89 | 11.86 | 19.14 | 51.83 |

Table S6

Kinetic curve fitting parameters for phosphate adsorption on SBP and SBP-La

| Biochar | Pseudo first-order model | | | Pseudo second-order model | | |
|---------|--------------------------|---------------|-------|---------------------------|---------------------|-------|
| | Q_{e1} (mg/g) | K_1 (/h) | R^2 | Q_{e1} (mg/g) | K_2 ((g/mg)/h) | R^2 |
| SBP | 7.42±0.30 | 0.247±0.027 | 0.913 | 7.62±0.30 | 0.317±0.004 | 0.977 |
| SBP-La | 39.1±1.1 | 0.310±0.042 | 0.897 | 45.6±0.9 | 0.942±0.103 | 0.978 |

Table S7

Isotherm curve fitting parameters for phosphate adsorption on SBP and SBP-La

| Biochar | Langmuir | | | Freundlich | | |
|---------|--------------------------|--------------------------|----------------|---|-------------|----------------|
| | Q ₀ (mg/g) | K _L (L/mg) | R ² | K _F ((mg/g)·(L/mg) ^{1/n}) | n | R ² |
| SBP | 7.67±0.37 | 2.85±0.18 | 0.981 | 6.27±0.26 | 0.045±0.010 | 0.680 |
| SBP-La | 46.5±0.31 | 0.413±0.065 | 0.923 | 32.3±2.5 | 0.004±0.015 | 0.774 |

Table S8

Thermodynamic curve fitting parameters for phosphate adsorption on SBP and SBP-La

| | Temperature (K) | ΔG ₀ (KJ/mol) | ΔH ₀ (KJ/mol) | ΔS ₀ (KJ/mol·K) |
|--------|-----------------|--------------------------|--------------------------|----------------------------|
| SBP | 298.0 | 4191 | 1330 | 1.031 |
| | 308.0 | 3349 | | |
| | 318.0 | 2727 | | |
| SBP-La | 298.0 | -2162 | 8790924 | 1.494 |
| | 308.0 | -3380 | | |
| | 318.0 | -4238 | | |

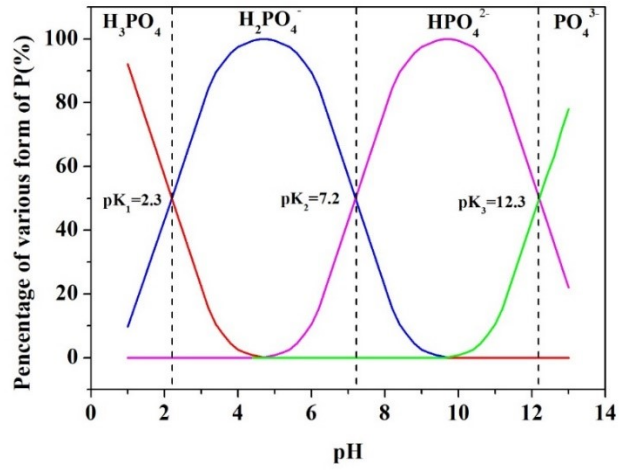


Fig. S1 Fractions of phosphate species at different pH²

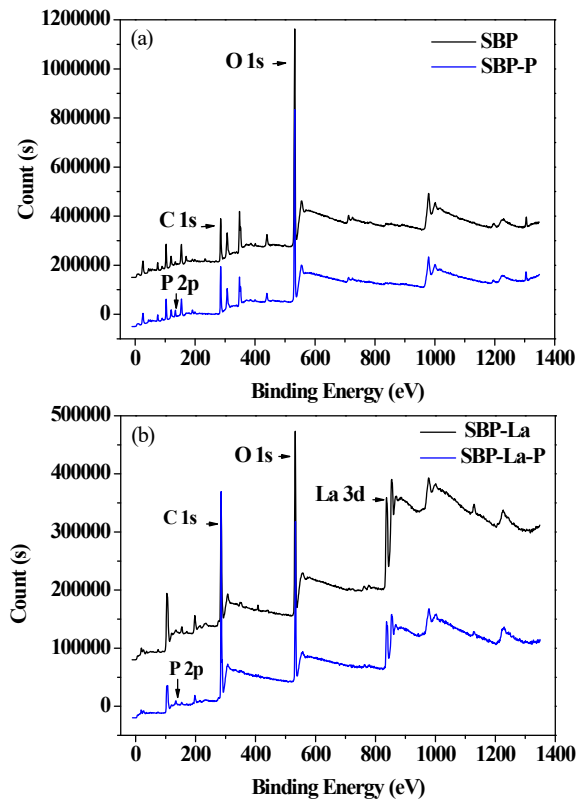


Fig. S2 XPS full spectrum of SBP (a) and SBP-La (b) before and after phosphate adsorption.

Reference

1. Y. Tang, J. Pan, B. Li, S. Zhao and L. Zhang, Residual and ecological risk assessment of heavy metals in fly ash from co-combustion of excess sludge and coal, *Sci Rep.*, 2021, **11**, 2499.
2. L. Liu, C. Zhang, S. Chen, L. Ma, Y. Li and Y. Lu, Phosphate adsorption characteristics of La(OH)₃-modified, canna-derived biochar, *Chemosphere*, 2022, **286**, 131773.
3. Y.-S. Ho and G. McKay, Pseudo-second order model for sorption processes, *Process Biochem.*, 1999, **34**, 451-465.
4. W. J. Weber and J. C. Morris, Kinetics of Adsorption on Carbon from Solution, *J. Sanit. Eng. Div.*, 1963, **89**, 31-59.
5. I. Langmuir, The adsorption of gases on plane surfaces of glass, mica and platinum, *J. Am. Chem. Soc.*, 1918, **40**, 1361-1403.
6. H. Freundlich, Uber die adsorption in lasugen (Leipzig), *Zeitschrift für Physikalische Chemie*, 1906, **57**, 385-470.